nature genetics

Accounting for genetic interactions improves modeling of individual quantitative trait phenotypes in yeast

Simon K G Forsberg[1], Joshua S Bloom[2–4], Meru J Sadhu[2–4], Leonid Kruglyak[2–4] & Örjan Carlborg[1]

© 2017 Nature America, Inc., part of Springer Nature. All rights reserved.

Experiments in model organisms report abundant genetic interactions underlying biologically important traits, whereas quantitative genetics theory predicts, and data support, the notion that most genetic variance in populations is additive. Here we describe networks of capacitating genetic interactions that contribute to quantitative trait variation in a large yeast intercross population. The additive variance explained by individual loci in a network is highly dependent on the allele frequencies of the interacting loci. Modeling of phenotypes for multilocus genotype classes in the epistatic networks is often improved by accounting for the interactions. We discuss the implications of these results for attempts to dissect genetic architectures and to predict individual phenotypes and long-term responses to selection.

When the combined phenotypic effect of alleles at two or more loci deviates from the sum of their individual effects, this is referred to as a genetic interaction, or epistasis. Most biological traits are regulated by a complex interplay between multiple genes and environmental factors. Despite this underlying complexity, data and theory have shown that it is expected that most of the genetic variance in a population will be additive[1–3]. The apparent contradiction between the complexity of the biological mechanisms that determine quantitative traits and the observation that most genetic variance can be captured by an additive model has led to a long-standing debate in genetics: does the predominant role of additive genetic variance mean that strictly additive models are always sufficient to describe the relationship between the genotype and the phenotype of an organism[1,4] or could there be added value in explicitly modeling genetic interactions despite the lower levels of epistatic genetic variance[5–8]?

There are some situations where data and theory have suggested that it might be particularly important to account for genetic interactions. One is when the aim is to predict the phenotypes of individuals on the basis of their genotype. If interactions lead to extreme phenotypes for some genotypes, these phenotypes are unlikely to be captured by additive models, particularly if they are rare. This has, for example, been illustrated for sporulation efficiency in yeast[9]. Another case is the prediction of long-term selection response. Under an additive model, both the additive variance and the response are expected to be nearly constant over the first few generations. As generations proceed, allele frequencies change to alter the additive variance and, consequently, the response to selection. This change is more rapid for traits regulated by fewer loci with larger effects than for traits regulated by many loci with smaller effects. It is known that genetic interactions can contribute to the additive genetic variance in a population[1,7]. The contribution, however, varies depending on the joint allele frequencies across all the interacting loci as well as on the types and strengths of the genetic interactions[10,11]. The changes in the additive variance, and hence the response, during ongoing selection are therefore more complex in the presence of genetic interactions. As a result, genetic interactions can make the long-term selection response more dynamic[12,13] and result in a realized response beyond predictions based on additive genetic effects and allele frequencies at individual loci[10,11]. However, as little is known about how prevalent and strong genetic interactions are in real populations and how much they contribute to the additive variance as allele frequencies change during selection, it has been difficult to obtain any empirically based conclusions about how influential these interactions are expected to be in these situations.

Here we analyze a panel of 4,390 yeast recombinant offspring (segregants) from a cross between a laboratory strain (BY) and a vineyard strain (RM), generated in Bloom *et al.*[3]. In this population, each segregant is genotyped for 28,220 SNPs and phenotyped for 20 endpoint growth traits. Across these traits, a total of 939 quantitative trait loci (QTLs) with additive effects and 330 QTLs with epistatic effects were mapped previously[3]. As the individuals in this population are haploids, the sample size is large and all allele frequencies are close to 50%, this data set presents a unique opportunity to accurately estimate how allelic combinations across large numbers of loci influence quantitative traits. Using phenotype information for multiple segregants with each possible allelic combination across many loci, we directly estimate how high-order genetic interactions contribute to complex trait variation in this segregating population. We quantify how well quantitative genetics models can capture the empirically identified relationships between multilocus genotypes and phenotypes.

We observe networks of epistatic loci for most of the traits in the study and find that some highly interactive loci in these networks can hide, or reveal, the effects of their interactors. We show that additive genetic models capture much of the genetic variance contributed by

[1]Department of Medical Biochemistry and Microbiology, Uppsala University, Uppsala, Sweden. [2]Department of Human Genetics, University of California, Los Angeles, Los Angeles, California, USA. [3]Howard Hughes Medical Institute, University of California, Los Angeles, Los Angeles, California, USA. [4]Department of Biological Chemistry, University of California, Los Angeles, Los Angeles, California, USA. Correspondence should be addressed to Ö.C. (orjan.carlborg@imbim.uu.se).

Received 28 October 2016; accepted 2 February 2017; published online 27 February 2017; doi:10.1038/ng.3800

the interacting genes in these networks. However, when these models are used to estimate the phenotypes for individual segregants, they often fail to fully capture the effects of multilocus genotypes that lead to extreme phenotypes. Accounting for interactions in the models led to more accurate phenotypic predictions for such genotypes. We illustrate this by analyzing an individual network in detail and then generalize the results across the other revealed networks. We discuss the potential impact of these findings on prediction of individual phenotypes, which is of importance in, for example, personalized medicine, prediction of long-term selection response in breeding and evolution, and interpretation of results from QTL and genome-wide association studies.

RESULTS

Many epistatic QTLs are part of highly connected networks

Most epistatic QTLs[3] interacted with one or a few loci, while a smaller subset were involved in pairwise interactions with several loci (**Fig. 1a**). By visualizing the 330 statistically significant epistatic QTLs[3] as nodes and the interactions between them as edges, we identified many networks of interacting loci. These networks were often connected with hub-and-spoke types of architectures where QTLs involved in many interactions tied larger networks together (**Fig. 1b**). We refer to these as radial networks, with a hub QTL in the center that connects the radial QTLs. Hub–radial QTL interactions were, on average, more significant than interactions that did not involve a hub QTL ($P = 3 \times 10^{-5}$, two-sided Wilcoxon test; **Supplementary Fig. 1**), supporting the idea that the radial architecture is a prominent feature of the networks. The available genotype and phenotype data allowed us to accurately estimate the phenotypes for individual six-locus genotype classes. We therefore selected the 15 six-locus radial networks where a hub QTL interacted with at least five other QTLs for further in-depth studies (**Fig. 1b**). The selected networks contributed to 11 of the 20 studied traits and included 81 QTLs.

Here we first illustrate our analyses and results for the network regulating growth on medium containing indoleacetic acid (IAA network) and then extend them to all networks.

Hub QTLs often moderate the phenotypic effects of radial QTLs

The hub QTL in the IAA network explained the most additive genetic variance of any locus for this trait ($\sigma_a^2/\sigma_p^2 = 11\%$), where σ_a^2 and σ_p^2 are the additive genetic and phenotypic variances, respectively). The phenotypic variance was threefold higher for segregants with the BY genotype than for segregants with the RM genotype at this locus. This heterogeneity in genetic variance is highly significant ($P < 2.2 \times 10^{-16}$; dglm, two-sided test). By estimating the narrow-sense heritability (h^2) separately among segregants with the BY and RM alleles at this hub QTL, we showed that much of this difference was due to genetics ($h^2_{BY} = 0.55$ vs. $h^2_{RM} = 0.14$). We here call such QTLs—where one allele suppresses genetic contributions by other loci and the other allele uncovers them—genetic capacitors. Across the 15 epistatic networks, 10 hub QTLs were genetic capacitors with significant differences in h^2 ($P < 0.001$, Bonferroni-corrected multiple-testing threshold, one-sided permutation test) between the genotypes ranging from 10% to 42%. By testing 40 randomly selected radial QTLs, we found that few ($n = 3$) of these were significant genetic capacitors and that they were weaker capacitors than the hubs (mean difference ± s.d. in h^2 for radial QTLs = 4.3 ± 3.6% vs. 12.5 ± 9.2% for hub QTLs). We also identified a strong correlation ($r = 0.64$, Pearson correlation; $P < 2.2 \times 10^{-16}$, two-sided test) between the level of heterogeneity in variance between the genotypes at the 330 epistatic QTLs and the number of interactions in which they were involved (**Supplementary Fig. 2**). Together, this shows that strong genetic capacitors[14,15] often are hubs in epistatic networks.

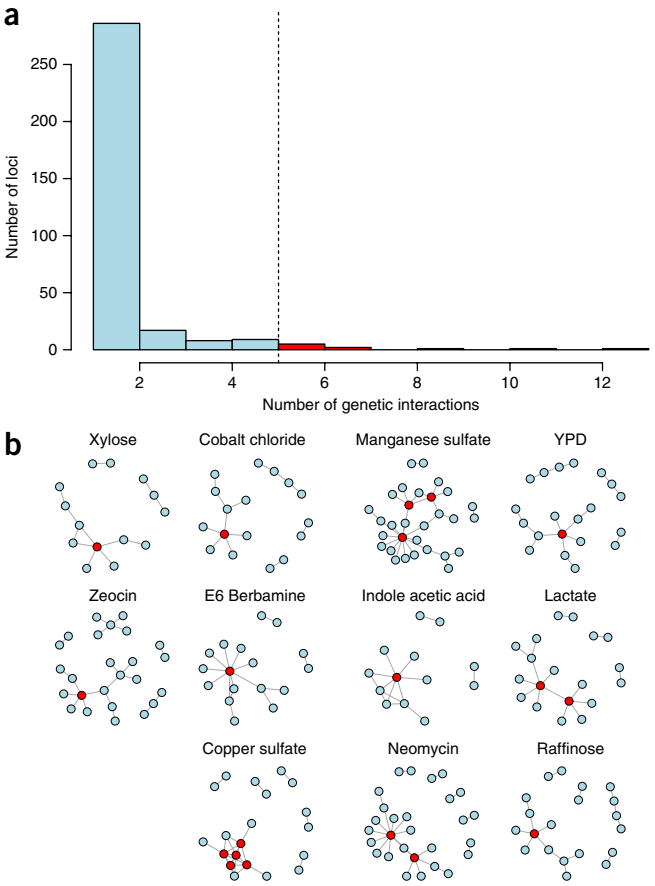

Figure 1 Many QTLs involved in pairwise interactions are part of highly interconnected epistatic networks. (**a**) A histogram of the number of interactions in which each epistatic QTL is involved. Most of the 330 epistatic loci detected for the 20 traits are involved in few pairwise interactions. Few QTLs are involved in many interactions, here defined as five or more, but their role is prominent because they are the hubs that tie the networks together. (**b**) The pairwise QTL interactions contributing to growth in 11 different media form highly interconnected epistatic networks. Each circle represents a QTL, and the lines represent significant pairwise interactions[3]. Red circles highlight hub QTLs involved in five or more pairwise interactions. YPD, yeast extract peptone dextrose.

Modeling phenotypes for multilocus genotype classes

Allelic interactions contribute to complex trait variation. For the six-locus IAA network, we divided the segregants into 64 groups representing each of the 64 possible six-locus genotype classes and calculated the phenotypic means and variances (**Fig. 2a**). Segregants with the capacitating BY allele at the hub QTL displayed the poorest growth when they had many IAA-sensitizing alleles at the five radial QTLs. In contrast, segregants with the canalizing RM allele at the hub QTL had similar growth regardless of how many IAA-sensitizing alleles they had at the radial QTLs. The RM and BY alleles at the hub QTL in the network thus decrease (canalize) and increase (capacitate) the effects of the radial QTLs, respectively (**Fig. 2a**). Similar results were also observed for several of the other networks with significant differences in h^2 between the genotypes at the hub QTL ($P < 0.001$, Bonferroni-corrected multiple-testing threshold, one-sided permutation test; **Supplementary Fig. 3**).

Across the networks, we detected hub QTL capacitor alleles of both BY and RM origin. The most extreme phenotypes in these networks were always observed for a genotype class with a combination of BY

© 2017 Nature America, Inc., part of Springer Nature. All rights reserved.

and RM alleles at the hub and radial loci. The alleles at the radial loci that required the presence of the capacitating hub allele to uncover their full effect on growth (**Fig. 3** and **Supplementary Figs. 3** and **4**) in 60% of the cases originated from the same strain as the canalizing hub allele. The two parental strains thus harbor cryptic, or hidden, genetic variation[16–19] whose phenotypic effect is revealed when combined in the haploid segregants.

Nonlinear capacitation effects in some epistatic networks. In the IAA network, the reduction in growth among the segregants with the BY allele at the hub QTL decelerated in a multiplicative, rather than a linear, manner as the number of IAA-sensitizing alleles increased (**Fig. 2b**). For segregants with the BY allele at the hub QTL, the effect of having five IAA-sensitizing alleles was much larger than five times the effect of having one IAA-sensitizing allele. As a result, an exponential model fit these data better than an additive model (R^2 increases from 0.34 to 0.39; **Fig. 2b**). One other network, affecting growth in medium containing copper sulfate, displayed a similar nonlinear capacitation (R^2 increased from 0.34 to 0.43; **Fig. 3d** and **Supplementary Fig. 4**). This multiplicative effect could result from measuring growth as the increase in radius of the yeast colonies or could be a feature of the underlying biology.

Extreme estimates from additive models are often biased. Many additive-model-based estimates of the phenotypes for multilocus genotype classes in the IAA network differed substantially from the actual values estimated directly from the data (**Fig. 2a**). Cross-validated model-based estimates were computed for each multilocus genotype class to quantify their accuracy and bias. Accuracy for each genotype class was measured by the mean square error (MSE), and bias was measured by the difference between the modeled and actual phenotypes. Twenty-three of the 64 estimates were significantly biased (Bonferroni-corrected multiple-testing threshold, $P < 0.05/64$, two-sided *t*-test), showing that the additive model was unable to represent the genetic contributions by the IAA network to many of the individual segregant phenotypes. To evaluate whether this trend generalized across all networks and whether alternative quantitative genetics model parameterizations could perform better, we fitted three different quantitative genetics models to all six-locus networks: (i) additive effects only, (ii) additive effects and pairwise interactions, and (iii) additive effects and pairwise and three-way interactions.

Models with only additive effects captured much of the phenotypic variance for all networks (on average, 28% of σ_p^2). Accounting for epistatic interactions only increased the variance explained marginally (on average, by 5% of σ_p^2). The additive-model-based estimates of the phenotypes were, however, significantly biased for between 1 and 23 of the 64 genotype classes per network in 14 of the 15 examined networks (Bonferroni-corrected multiple-testing threshold, $P < 0.05/64$, two-sided *t*-test; **Figs. 2** and **4**, and **Supplementary Fig. 5**). Models with pairwise interaction terms provided unbiased estimates of all 64 measured genotype values for most networks. Only two networks required three-way interaction terms to remove all detectable bias. In 5 of the 15 networks, the accuracy was significantly better for at least 1 of the 64 genotype classes when using models with pairwise interaction terms (Bonferroni-corrected multiple-testing threshold, $P < 0.05/64$, two-sided *t*-test; **Supplementary Fig. 6**).

The bias for the additive model estimates of the phenotypes of individual multilocus genotypes was largest for the most extreme trait values, that is, those corresponding to the best or worst growth in the capacitated group and the best or worst estimated growth in the canalized group (**Figs. 2** and **4**). In networks where the hub QTLs were capacitors, the direction of the bias depended on

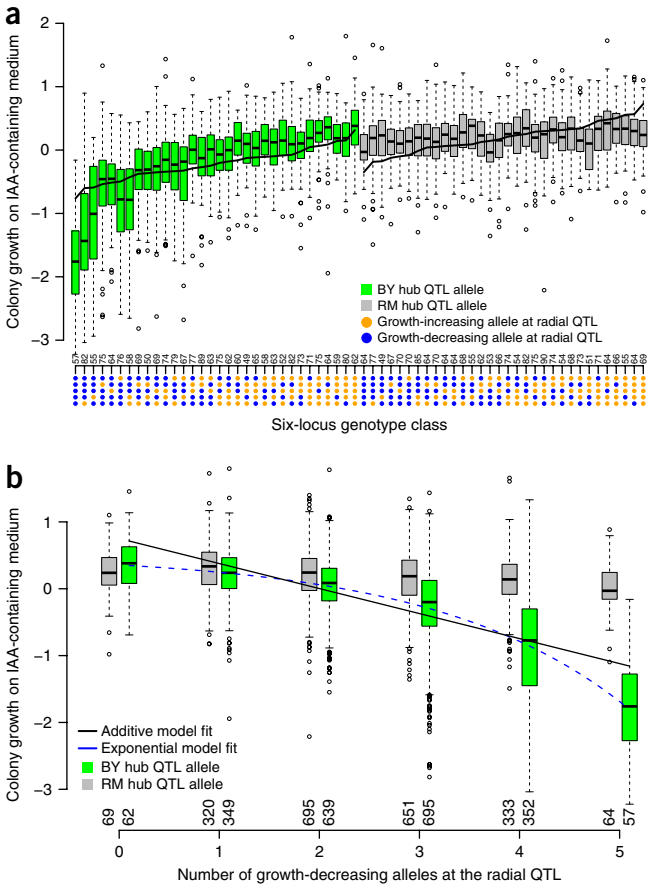

Figure 2 Epistatic network regulating growth on IAA-containing medium. The RM allele suppresses (canalizes) the phenotypic effects of segregating alleles at the radial QTLs. The BY allele capacitates the growth-decreasing effects that combine in a nonlinear fashion. Tukey box plots (where the bottom and top of the box are the first and third quartiles, the band is the median and the whiskers extend to the lowest and highest data points within 1.5 times the interquartile range) illustrate the phenotypic distributions in segregants with different combinations of alleles across the IAA network. (**a**) A box plot is shown for each of the 64 genotype classes. Color indicates the genotype at the hub QTL (chrVIII: 114,114 bp; green and gray boxes correspond to BY and RM alleles, respectively). The *x* axis gives the six-locus genotype class, where blue and orange dots indicate growth-decreasing and growth-increasing alleles at the five radial QTLs (from top to bottom: chrXIV: 469,224 bp, chrIII: 198,615 bp, chrIV: 998,628 bp, chrXIII: 410,320 bp, chrXII: 645,539 bp). The black line through the boxes illustrates the additive-model-based estimates of the phenotypes for the 64 genotype classes. The number above the *x* axis is the number of segregants in each genotype class. (**b**) A box plot is shown for each group of segregants that have the same number of growth-decreasing alleles at the five radial QTLs. The segregants are divided and colored on the basis of genotype at the hub QTL as in **a**. The *x* axis gives the number of growth-decreasing alleles at the radial QTLs and the number of segregants in each group. The regression lines illustrate the fit for linear additive (black; $R^2 = 0.34$) and nonlinear exponential (dashed blue; $R^2 = 0.39$) models.

the genotype at the capacitor: Among segregants with the capacitor allele at the hub QTL, the models underestimated the phenotypic effect of combining many growth-increasing or growth-decreasing alleles at the radial QTLs (**Fig. 4a**). For segregants with the canalizing allele at the hub QTL, the models instead overestimated these phenotypic effects (**Fig. 4b**). By accounting for epistatic interactions, the bias was reduced or entirely removed (**Fig. 4**). For the five networks

© 2017 Nature America, Inc., part of Springer Nature. All rights reserved.

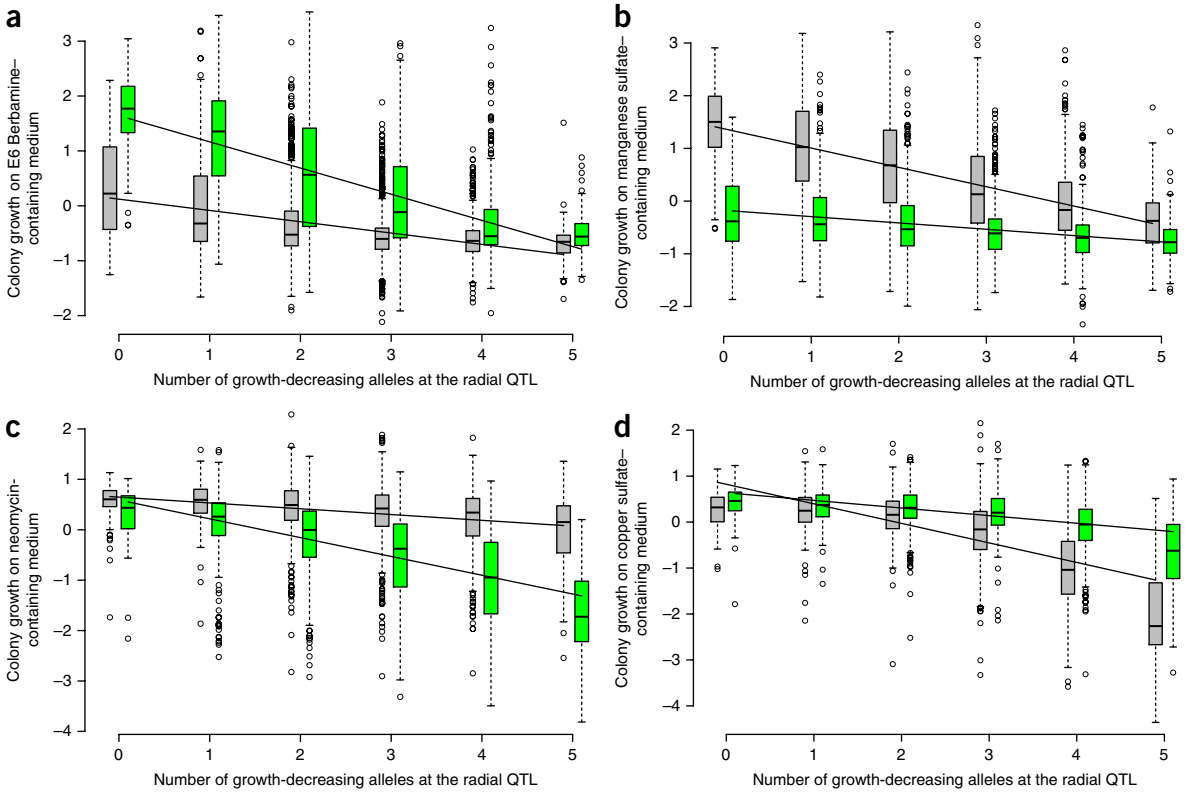

Figure 3 Epistatic networks contain hub QTL capacitor alleles of both BY and RM origin that moderate growth-increasing or growth-decreasing effects of segregating alleles at radial QTLs. (**a**–**d**) Each panel corresponds to one epistatic network where the hub QTL capacitates the growth-increasing or growth-decreasing effects of segregating alleles at the radial QTLs: E6 Berbamine (**a**), manganese sulfate (**b**), neomycin (**c**) and copper sulfate (**d**). Within each network, the segregants are divided on the basis of genotype at the hub QTL: segregants carrying the RM allele are shown in gray, and those with the BY allele are shown in green. The *x* axis gives the number of growth-decreasing alleles at the radial QTLs. The Tukey box plots (where the bottom and top of the box are the first and third quartiles, the band is the median and the whiskers extend to the lowest and highest data points within 1.5 times the interquartile range) show phenotypic distributions for groups of segregants with different numbers of growth-affecting alleles at the five radial QTLs in six-locus epistatic networks. (**a**,**b**) Networks where the RM (BY) allele at the hub QTL maintains low growth in the segregants almost regardless of the genotypes at the radial QTLs. (**c**,**d**) The RM (BY) alleles allow the segregants to maintain high growth almost regardless of which alleles segregate at the radial QTLs. The regression lines illustrate the difference in effects of the radial QTL alleles depending on the genotype at the hub QTL.

where the hub QTL was not a significant capacitor, the bias was not dependent on the genotype at the hub QTL.

Genetic variances explained by loci in epistatic networks

The additive genetic variance contributed by a locus depends on its effect and allele frequency in the analyzed population[20]. When loci interact, the variance explained marginally by each of the epistatic loci will in addition also depend on the frequencies at the loci with which it interacts. For example, the additive genetic variance contributed by each individual locus in the IAA network varied depending on the allele frequencies of all loci in the network owing to the extensive interactions among the loci. When considering the entire population of segregants (all allele frequencies ~0.5), the additive variance (σ^2_p) contributed by the network amounted to 26.8% of the total phenotypic variance in the population. In the subpopulations where the BY or RM alleles at the hub QTL were fixed (BY allele frequency = 1 or 0), the network instead contributed 36% and 3% of the total phenotypic variance, respectively. To generalize this result across the allele frequency space, we simulated populations with allele frequencies ranging from 0.05 to 0.95 at increments of 0.15 for the six loci in the network. We then evaluated how the additive genetic variance contributed by the individual loci varied depending on the allele frequencies at the other five loci. We also simulated populations without genetic interactions. In **Figure 5**, we summarize the results for the simulations based on the 64 actual genotype values in the IAA network. The additive genetic variance contributed by the hub QTL varied from 0% to 58% of the total phenotypic variance in the population, only by changing the allele frequencies at the five other loci (**Fig. 5**). The result was similar for the other five QTLs, although their ranges were smaller than for the hub QTL (**Fig. 5**, blue boxes; average range: 0% to 31% of σ^2_p). As expected, the additive genetic variance contributed by each locus was much less dependent on the allele frequencies when loci with the same marginal effects, but no interactions, were simulated (**Fig. 5**, red boxes; range: 2% to 6% of σ^2_p). The results were similar across all 15 networks, with estimates of additive genetic variance for individual epistatic loci that were highly dependent on the allele frequencies at the other loci in the network.

DISCUSSION

The link between the genotype and the phenotype of an organism is immensely complex. Despite this complexity, the link can, to a great extent, be captured using models that assume that gene variants combine their effects in an additive manner. Here we used a large experimental yeast cross to identify six-locus epistatic networks affecting

© 2017 Nature America, Inc., part of Springer Nature. All rights reserved.

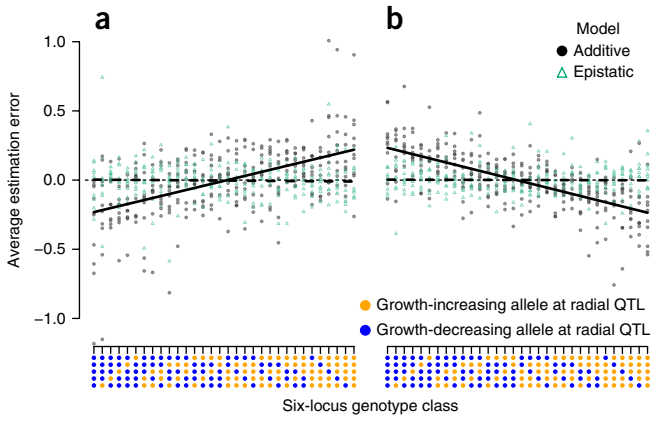

Figure 4 Biases in additive-model-based estimates of phenotypes are largest in the genotype classes with the greatest or poorest expected growth. Across the ten interaction networks with a capacitor hub QTL, the most extreme additive-model-based representations of individual multilocus genotypes are biased. The additive model under- or overestimates the extremity of the genotypes with many or few growth-decreasing alleles at the radial QTLs, respectively. (**a**) This results in a positive correlation between the estimation errors (bias) and the number of growth-increasing alleles at the radial QTLs when there is a capacitor allele at the hub QTL ($r = 0.54$, Pearson correlation; $n = 320$; $P < 2.2 \times 10^{-16}$, two-sided test). (**b**) Among segregants with a non-capacitor allele at the hub QTL, the trend is the opposite with over- and underestimates for segregants with many and few growth-decreasing alleles at the radial QTLs ($r = -0.69$, Pearson correlation; $n = 320$; $P < 2.2 \times 10^{-16}$, two-sided test). The *y* axis gives the average estimation error (bias) from cross-validation for each genotype in the ten networks. The *x* axis illustrates the genotype at the five radial QTLs in the networks: blue and orange dots indicate growth-increasing and growth-decreasing alleles, respectively. Each dot represents the average estimation error (bias) for a particular six-locus genotype class in one of the ten networks. Black dots (green triangles) are errors from additive-only (additive + pairwise interaction) models with solid (dashed) black lines denoting the regression on these errors. The estimation errors (biases) are calculated as measured – estimated phenotypes, and over- and underestimations will therefore result in negative and positive estimation errors (biases), respectively.

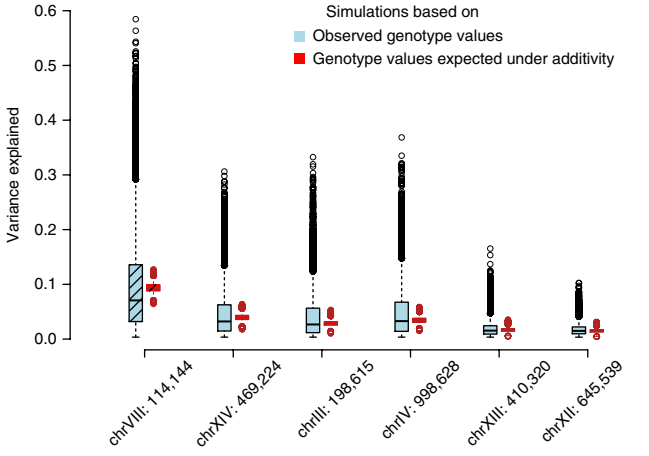

Figure 5 Simulations show that the additive genetic variances contributed by the loci in the epistatic network regulating growth on IAA-containing medium are highly dependent on the allele frequencies at the other loci in the same network. The phenotypic variance explained by the individual loci in the IAA network depends on the allele frequencies at the other loci with which they interact. Each Tukey box plot (where the bottom and top of the box are the first and third quartiles, the band is the median and the whiskers extend to the lowest and highest data points within 1.5 times the interquartile range) shows the additive genetic variances across 16,807 simulated populations. For each locus, we simulated populations where the allele frequencies of the loci themselves were fixed at 0.5 while varying the frequencies at the other five loci from 0.05 to 0.95 in increments of 0.15. The light blue boxes represent the variability in the additive genetic variances when simulating populations on the basis of the observed phenotypic means for the 64 genotype classes in the IAA network. The red boxes represent the additive genetic variances when simulating on the basis of the phenotypic means estimated using the additive genetic model (black line in **Fig. 2a**). The *x* axis gives the location of the SNP representing each locus (chromosome: location in base pairs). The two leftmost box plots (diagonal lines) show the simulation results for the hub QTL.

11 complex traits. We then estimated the average phenotypes for the groups of segregants sharing each combination of alleles at these loci. We evaluated how well different quantitative genetics models captured the phenotypes of these multilocus genotype classes. In most networks, the phenotypes for at least one, but often several, multilocus genotype classes deviated significantly from what is expected under an additive model. This empirically illustrates the important role of classic epistasis, as defined by Bateson more than 100 years ago[21], in the genetic architecture of complex traits. We provide several examples of such epistasis, involving multiple loci in highly interconnected genetic networks.

An earlier study of this population[3] showed that most of the genetic variance for the 20 measured traits is additive. Consistent with this, the additive-model-based estimates of the phenotypes for most multilocus genotype classes in the epistatic networks were reasonable. However, the most extreme estimates from the additive models were often both inaccurate and biased (**Fig. 4**). For example, the bias is very large for the most extreme genotype class in the IAA network ($1.7\ \sigma_p$; **Fig. 2**). Our results highlight the importance of analyzing collected data with models that can represent the features of the underlying genetic architectures. They also confirm that, regardless of the underlying genetic architecture, additive models are likely to capture much of the genetic variation for a trait. This makes them useful for identifying genes contributing to the phenotypic variance in a particular population, as well as for predicting short-term response to selection in a population[11]. However, we also show that additive models are often unable to represent all key features of genetic architectures involving networks of epistatic loci. In particular, their most extreme estimates are often inaccurate and biased for networks with capacitor hub QTLs. Accounting for epistasis increases estimation accuracy and decreases bias. Modeling genetic interactions should therefore be considered when it is important to identify and predict the effects of specific combinations of alleles or where it is important to identify genotypes that are likely to lead to extreme phenotypes. Examples of this include prediction of disease risk or drug responses in individual patients.

As shown here and in earlier studies[1,7,22], most genetic variance in a population is expected to be additive even in the presence of extensive epistasis. The lack of empirical knowledge about the pervasiveness and strength of epistasis in the genetic architectures of complex traits makes it largely unknown how much of the observed additive genetic variance in quantitative genetics studies is due to genetic interactions. This experimental yeast population allowed us to directly estimate the phenotypes for individual multilocus genotype classes in networks of interacting loci. With these as a basis, we used simulations to demonstrate that the types of interactions shown here have a very large influence on both estimates of the additive genetic effects

© 2017 Nature America, Inc., part of Springer Nature. All rights reserved.

of the individual loci and their contributions to the additive genetic variance. The IAA network provides a striking example: the additive variance contributed by the hub QTL in the epistatic network (**Fig. 2**) ranged from zero to the largest contribution by any single locus across all networks when we varied the allele frequencies at the five radial QTLs. This empirically illustrates how allelic interactions (epistasis) can be the main driver of the additive genetic variance in a population and that the importance of epistasis in the genetic architecture of a complex trait cannot be inferred from the relative levels of additive and epistatic genetic variance.

Many interacting loci in this population were part of radial epistatic networks where hub loci interact with multiple other QTLs. In general, this network topology reflected how the loci contributed to the phenotypic variation in the population. The hub QTLs acted as genetic capacitors that modified the effects of the radial loci in the network. These capacitating interactions are highly influential for the total level of phenotypic variance displayed in a population, as they can both buffer and release cryptic (standing) genetic variation[23,24]. Several genetic capacitors have been studied in molecular detail, including the heat shock protein *HSP90* (refs. 16,25) and *EGFR*[26]. Genetic capacitation has also been found for complex traits in segregating populations. For example, it facilitated extreme selection responses for body weight in a long-term experimental selection experiment in chicken[10–12] and contributed to the variation in root length among natural *Arabidopsis thaliana* accessions[27]. This study suggests that capacitor networks are likely to be a common property of the genetic architecture of complex traits. We found them to be both common and influential for many traits in this population, suggesting that they should be considered in other studies of complex traits, including those aiming to genetically dissect or statistically predict responses to long-term selection.

It is currently unknown how IAA affects yeast fitness, but the discovery of the epistatic network described here may shed some light on its mode of action. The hub QTL in the IAA network maps to the gene *GPA1*, which is required for the yeast response to mating pheromone. Although this response is not normally triggered under laboratory growth conditions, as the yeast is not exposed to mating pheromone, the BY allele of *GPA1* leads to residual expression of the pheromone response pathway[28,29]. Thus, a model for the capacitance activity of the BY allele of *GPA1* is that IAA primarily affects cells with an activated pheromone response pathway. Interacting radial QTLs would then arise if the underlying variants influence either the response to IAA or activation of the pheromone response pathway by the BY allele of *GPA1*. The radial QTLs include several loci involved in pheromone response, including the mating-type locus *MAT*, which dictates which pheromones are expressed or sensed (and is known to interact with *GPA1*)[30], and the gene *VPS34*, which is required for the activation by *GPA1* of the mating pathway[31]. Further work will be required to elucidate the importance of the yeast pheromone response pathway for the fitness effects of IAA.

For several other networks, the hub QTLs include candidate genes with known polymorphisms in BY and RM. For example, the networks regulating growth on media with copper sulfate and manganese sulfate have hub QTLs that include the genes *CUP1* and *PMR1*, respectively. The BY allele of *CUP1* (ref. 32) is known to increase copper ion tolerance[33], and the RM allele of *PMR1* confers manganese resistence[34]. The current data do not allow further functional dissection of the possible connections between these polymorphisms and the capacitation in the networks. However, by showing the allelic dependencies between the loci in the network (**Fig. 3b**,**d**), it is possible to formulate hypotheses about how these and other known polymorphisms in hub QTLs could contribute epistatically to growth in the respective media for testing in future functional studies (**Supplementary Note**).

In summary, we show that networks of capacitating genetic interactions are common and that these networks form a key part of the genetic architectures of multiple complex traits in a large experimental yeast population. We illustrate how such interactions affect model-based estimation of individual phenotypes and the inference of genetic architectures. This shows that epistasis needs to be explored beyond estimates of epistatic genetic variances, to understand its contribution to the phenotypic variability and long-term selection responses in populations. This is a key discovery in the long-standing debate about how to approach epistasis in complex trait research.

URLs. R Project for Statistical Computing (accessed 17 January 2017), http://www.r-project.org/; dglm: Double Generalized Linear Models (accessed 17 January 2017), https://cran.r-project.org/web/packages/dglm/.

METHODS

Methods, including statements of data availability and any associated accession codes and references, are available in the online version of the paper.

Note: Any Supplementary Information and Source Data files are available in the online version of the paper.

ACKNOWLEDGMENTS

Funding was provided by the Howard Hughes Medical Institute and by NIH grants R01 GM102308 (L.K.) and F32 GM116318 (M.J.S.) and Swedish Research Council grant 621-2012-4632 (Ö.C.).

AUTHOR CONTRIBUTIONS

Analyses were designed by S.K.G.F., J.S.B., M.J.S., L.K. and Ö.C. Analyses were conducted by S.K.G.F. and Ö.C. The manuscript was written by S.K.G.F. and Ö.C. and incorporates comments by J.S.B., M.J.S. and L.K.

COMPETING FINANCIAL INTERESTS

The authors declare no competing financial interests.

Reprints and permissions information is available online at http://www.nature.com/reprints/index.html.

1. Hill, W.G., Goddard, M.E. & Visscher, P.M. Data and theory point to mainly additive genetic variance for complex traits. *PLoS Genet.* **4**, e1000008 (2008).
2. Bloom, J.S., Ehrenreich, I.M., Loo, W.T., Lite, T.-L.V. & Kruglyak, L. Finding the sources of missing heritability in a yeast cross. *Nature* **494**, 234–237 (2013).
3. Bloom, J.S. *et al.* Genetic interactions contribute less than additive effects to quantitative trait variation in yeast. *Nat. Commun.* **6**, 8712 (2015).
4. Polderman, T.J.C. *et al.* Meta-analysis of the heritability of human traits based on fifty years of twin studies. *Nat. Genet.* **47**, 702–709 (2015).
5. Cheverud, J.M. & Routman, E.J. Epistasis and its contribution to genetic variance components. *Genetics* **139**, 1455–1461 (1995).
6. Carlborg, O. & Haley, C.S. Epistasis: too often neglected in complex trait studies? *Nat. Rev. Genet.* **5**, 618–625 (2004).
7. Mackay, T.F.C. Epistasis and quantitative traits: using model organisms to study gene–gene interactions. *Nat. Rev. Genet.* **15**, 22–33 (2014).
8. Nelson, R.M., Pettersson, M.E. & Carlborg, Ö. A century after Fisher: time for a new paradigm in quantitative genetics. *Trends Genet.* **29**, 669–676 (2013).
9. Gerke, J., Lorenz, K. & Cohen, B. Genetic interactions between transcription factors cause natural variation in yeast. *Science* **323**, 498–501 (2009).
10. Le Rouzic, A., Siegel, P.B. & Carlborg, O. Phenotypic evolution from genetic polymorphisms in a radial network architecture. *BMC Biol.* **5**, 50 (2007).
11. Le Rouzic, A. & Carlborg, Ö. Evolutionary potential of hidden genetic variation. *Trends Ecol. Evol.* **23**, 33–37 (2008).
12. Carlborg, O., Jacobsson, L., Ahgren, P., Siegel, P. & Andersson, L. Epistasis and the release of genetic variation during long-term selection. *Nat. Genet.* **38**, 418–420 (2006).
13. Paixão, T. & Barton, N.H. The effect of gene interactions on the long-term response to selection. *Proc. Natl. Acad. Sci. USA* **113**, 4422–4427 (2016).
14. Rönnegård, L. & Valdar, W. Detecting major genetic loci controlling phenotypic variability in experimental crosses. *Genetics* **188**, 435–447 (2011).
15. Rönnegård, L. & Valdar, W. Recent developments in statistical methods for detecting genetic loci affecting phenotypic variability. *BMC Genet.* **13**, 63 (2012).

© 2017 Nature America, Inc., part of Springer Nature. All rights reserved.

16. Rutherford, S.L. & Lindquist, S. Hsp90 as a capacitor for morphological evolution. *Nature* **396**, 336–342 (1998).
17. True, H.L. & Lindquist, S.L. A yeast prion provides a mechanism for genetic variation and phenotypic diversity. *Nature* **407**, 477–483 (2000).
18. Gibson, G. & Dworkin, I. Uncovering cryptic genetic variation. *Nat. Rev. Genet.* **5**, 681–690 (2004).
19. Paaby, A.B. & Rockman, M.V. Cryptic genetic variation: evolution's hidden substrate. *Nat. Rev. Genet.* **15**, 247–258 (2014).
20. Falconer, D.S. & Mackay, T.F.C. *Introduction to Quantitative Genetics* 4th edn (Longmans Green, 1996).
21. Bateson, W. Facts limiting the theory of heredity. *Science* **26**, 649–660 (1907).
22. Monnahan, P.J. & Kelly, J.K. Epistasis is a major determinant of the additive genetic variance in *Mimulus guttatus*. *PLoS Genet.* **11**, e1005201 (2015).
23. Bergman, A. & Siegal, M.L. Evolutionary capacitance as a general feature of complex gene networks. *Nature* **424**, 549–552 (2003).
24. Masel, J. & Siegal, M.L. Robustness: mechanisms and consequences. *Trends Genet.* **25**, 395–403 (2009).
25. Queitsch, C., Sangster, T.A. & Lindquist, S. Hsp90 as a capacitor of phenotypic variation. *Nature* **417**, 618–624 (2002).
26. Dworkin, I., Palsson, A., Birdsall, K. & Gibson, G. Evidence that *Egfr* contributes to cryptic genetic variation for photoreceptor determination in natural populations of *Drosophila melanogaster*. *Curr. Biol.* **13**, 1888–1893 (2003).
27. Lachowiec, J., Shen, X., Queitsch, C. & Carlborg, Ö. A genome-wide association analysis reveals epistatic cancellation of additive genetic variance for root length in *Arabidopsis thaliana*. *PLoS Genet.* **11**, e1005541 (2015).
28. Yvert, G. *et al. Trans*-acting regulatory variation in *Saccharomyces cerevisiae* and the role of transcription factors. *Nat. Genet.* **35**, 57–64 (2003).
29. Lang, G.I., Murray, A.W. & Botstein, D. The cost of gene expression underlies a fitness trade-off in yeast. *Proc. Natl. Acad. Sci. USA* **106**, 5755–5760 (2009).
30. Brem, R.B., Storey, J.D., Whittle, J. & Kruglyak, L. Genetic interactions between polymorphisms that affect gene expression in yeast. *Nature* **436**, 701–703 (2005).
31. Slessareva, J.E., Routt, S.M., Temple, B., Bankaitis, V.A. & Dohlman, H.G. Activation of the phosphatidylinositol 3-kinase Vps34 by a G protein α subunit at the endosome. *Cell* **126**, 191–203 (2006).
32. Fogel, S., Welch, J.W. & Maloney, D.H. The molecular genetics of copper resistance in *Saccharomyces cerevisiae*—a paradigm for non-conventional yeasts. *J. Basic Microbiol.* **28**, 147–160 (1988).
33. Perlstein, E.O., Ruderfer, D.M., Roberts, D.C., Schreiber, S.L. & Kruglyak, L. Genetic basis of individual differences in the response to small-molecule drugs in yeast. *Nat. Genet.* **39**, 496–502 (2007).
34. Sadhu, M.J., Bloom, J.S., Day, L. & Kruglyak, L. Mapping without crosses. *Science* **352**, 1113–1116 (2016).

© 2017 Nature America, Inc., part of Springer Nature. All rights reserved.

ONLINE METHODS

The creation of the BY × RM cross, genotyping, phenotyping, quality control of genotypes, filtering and normalization of growth measurements have previously been described in refs. 2,3. The reanalyzed data are available as supplementary information in ref. 3. Additive QTLs were mapped in ref. 3. All analyses were performed using the R framework for statistical computing (see URLs). All figures were prepared using R.

Statistical analysis. *Inferring epistatic networks.* Pairwise epistatic interactions were mapped by Bloom *et al.*[3]. Networks of epistatic loci were inferred by connecting loci that displayed pairwise interactions. The R package igraph[35] was used to visualize individual networks and to identify network hubs. The genome-wide association analysis for growth on IAA-containing medium among the segregants with the BY allele at the hub locus was performed using the qtscore function in the R package GenABEL[36]. Genome-wide significance was determined using a Bonferroni-corrected significance threshold for the number of tested markers ($P < 0.05/28{,}220 = 1.8 \times 10^{-6}$). The additive genetic variance explained by a certain set of QTLs was calculated as the R^2 value from a fixed-effect model without interactions.

Exhaustive mapping of loci in the network affecting growth on IAA-containing medium. To identify all individual loci that contributed the additional genetic variance among the segregants carrying the BY allele at the hub QTL in the IAA network, we performed a genome-wide association analysis in this group of segregants using the qtscore function in GenABEL[36] with significance thresholds as described above. This identified eight genome-wide significant loci in the radial network, of which six were the same as the loci in the earlier two-way interaction analysis[3].

Estimating average phenotypes for multilocus genotypes. Average phenotypes were estimated for each of the $2^6 = 64$ possible combinations of alleles for 15 six-locus epistatic networks. Each of these networks had a hub QTL connected to five radial loci by pairwise interactions. On average, $4{,}390/64 \approx 69$ segregants are expected in each six-locus genotype class in these networks, allowing confident estimation of the average growth associated with carrying each possible combination of alleles at these loci (exact values in each class are reported in the figures describing the results). Some of the hub QTLs were connected to more than five other loci in the network in the initial network analysis. Here we only kept the loci with the strongest statistical interaction with the hub QTL, as we could not confidently estimate phenotypes for individual genotype classes in networks with more than six loci.

Estimation of the genetic variance heterogeneity at a locus. We estimated the difference in the phenotypic variance between segregants that carry alternative alleles at the epistatic loci using a double generalized linear model (DGLM)[37], as suggested in Rönnegård *et al.*[14]. This allowed us to simultaneously model the effects of every locus on the phenotypic mean and variance. We fitted a DGLM with linear predictors for both mean and variance as $y \sim N(\mu_1 + X\beta_1, e^{\mu_2 + X\beta_2})$ using the R package dglm (see URLs) where y is the phenotype, X is the genotype, β_1 is the effect on the mean and β_2 is the effect on the variance. Coding the genotypes in X as 0 and 1, β_1 then describes the difference in mean whereas e^{β_2} describes the fold difference in variance between the segregants with alternative alleles at the locus.

Estimating the capacitating effects of the hub QTL in the epistatic networks. QTLs interacting with five or more other loci were defined as hubs. We estimated the capacitating effects of all hub QTLs as follows. For each network containing a hub QTL, we divided the segregants into two groups on the basis of their genotype at the hub QTL. We then fitted the mixed model $y = X\mu + a + e$ separately for each group. Here y is a column vector containing the phenotypes, X is a column vector of ones, μ is the overall mean, $b \sim N(0, A\sigma_a^2)$ and $e \sim N(0, \sigma_e^2)$. A is the additive kinship matrix, giving the fraction of the genome shared for each pair of segregants, σ_a^2 is the additive genetic variance captured by the markers and σ_e^2 is the residual variance. A was calculated using the ibs function in the R package GenABEL[36]. We used the GenABEL function polygenic to fit the mixed model. The narrow-sense heritability in each group was calculated as the within-class correlation.

$$\rho = \frac{\sigma_a^2}{\sigma_a^2 + \sigma_e^2}$$

We performed a permutation test to obtain the significance of the difference $\rho_1 - \rho_2$ between the two groups of segregants in each network. For each of the 20 traits, we randomly divided the population into two groups and estimated ρ_1 and ρ_2 in these groups as described above. This was repeated 1,000 times for each trait to obtain 20 empirical null distributions. We here report the number of traits for which the difference $\rho_1 - \rho_2$ was significant at a Bonferroni-corrected multiple-testing threshold of $0.05/15 \approx 0.003$.

Quantifying nonlinear effects after capacitation. To quantify the potential nonlinear effects of capacitated radial alleles, we compared the fit of an additive ($y = \mu + x\beta + e$) model and an exponential ($y = \mu + \beta_1 e^{x\beta_2} + e$) model. Here y is the phenotype, x is the number of growth-decreasing radial QTL alleles and e is the residual variance.

Modeling the phenotypes for individual multilocus genotype classes. For each six-locus epistatic network, we estimated the phenotypes for the 64 individual genotype classes in each network using three different models, including (i) additive effects, (ii) additive effects and pairwise interactions and (iii) additive effects and pairwise and three-way interactions. For (ii) and (iii), the included interaction terms, together with all additive terms, minimized $\mathrm{AIC} = 2k - 2\ln(L)$. Here k is the number of included parameters and L is the maximum-likelihood value for the model. We used the R function step in the stats package to perform the backward elimination. The performance of the final models (bias and accuracy) was evaluated using tenfold cross-validation where the variable selection for (i) and (ii) was performed within the training data in every fold.

Within each of the 64 genotype classes, defined by the six loci in each network, we calculated the cross-validation estimation errors as $e = y - \hat{y}$. Here y is the actual and $\hat{y}$ is the estimated phenotype. We tested whether e significantly deviated from 0 using a t-test. If the deviation was significant at a multiple-testing Bonferroni-corrected threshold of $0.05/64 \approx 7.8 \times 10^{-4}$, we considered the estimate for that particular genotype class to be biased. The accuracy of the estimates was measured by e^2, and for each genotype class we tested the difference in e^2 between models with and without interaction terms using a t-test. If e^2 was significantly lower for the interaction model, at a multiple-testing Bonferroni-corrected threshold of $0.05/64 \approx 7.8 \times 10^{-4}$, we considered these estimates to be more accurate.

Simulations. In the simulations, we used the phenotypic means $\mu_1, \ldots, \mu_{64}$ in each of the $2^6 = 64$ classes for each of the 15 six-locus networks and the total phenotypic variance σ_p^2 for each trait, obtained in the analyses above as a representation of the genetic architectures of these traits. In every simulation, we generated populations with the same number of segregants as in the original data set ($n = 4{,}390$). The number of segregants in each genotype class was determined by the allele frequencies $p_1, \ldots, p_6$ at the six loci. For example, the number of observations with genotype ABcDef, where capital and lowercase letters indicate the alternative alleles at the six loci, would be $p_1 \times p_2 \times (1 - p_3) \times p_4 \times (1 - p_5) \times (1 - p_6) \times n$. To evaluate the effect of different combinations of allele frequencies at the loci on the results, we simulated populations with $p_k \in \{0.05, 0.20, 0.35, 0.50, 0.65, 0.80, 0.95\}$, where $k = 1, \ldots, 6$. This leads to, in total, 7^6 allele frequency combinations. The phenotypes for the individuals in each genotype class were then simulated as $y_k \sim N(\mu_k, \sigma_p^2)$, where $k = 1, \ldots, 64$ and σ_p^2 is the total phenotypic variance for the trait.

As a comparison, we also simulated populations where the genetic architectures (i.e., the phenotype for each of the 64 multilocus genotypes) for the 15 networks were given by the estimates obtained from a six-locus additive model fitted to the respective loci. The linear model used was $y = X\beta + e$, where y is a column vector containing the phenotypes, X is a $4{,}390 \times 7$ matrix with column 1 consisting of ones and columns 2–7 consisting of the genotypes of the six loci, β is a 1×7 column vector with intercept and additive genetic effects, and e is the residual variance. Using this model, estimates $\widehat{\mu_1}, \ldots, \widehat{\mu_{64}}$ were obtained for each genotype class. The simulations were then performed across the different combinations of allele frequencies as described above, with phenotypes given by $y_k \sim N(\widehat{\mu_k}, \sigma_p^2)$.

The additive genetic variance contributed by each locus was estimated as the R^2 value from the linear model $y = X\beta + e$, fitted to the respective subset of the 7^6 simulated populations where the allele frequency of the locus itself was 0.5 ($p_1 = 0.5$) and the frequency at the other five loci varied in

© 2017 Nature America, Inc., part of Springer Nature. All rights reserved.

doi:10.1038/ng.3800

$p_k \in \{0.05, 0.20, 0.35, 0.50, 0.65, 0.80, 0.95\}$, where $k = 2, \ldots, 6$. In this model, X is a column vector with the genotype of the locus whose allele frequency is 0.5. The additive genetic variances were estimated in such subsets to analyze the effect of the individual locus across variable genetic backgrounds for the other loci, without the estimates being influenced by changes to the allele frequency of the analyzed locus itself.

Code availability. The custom R code for the analyses and simulations in the manuscript has been deposited in GitHub and is available at https://github.com/simfor/yeast-epistasis-paper.

Data availability. The genotype and phenotype data that were reanalyzed in this study are available in the supplementary information of the original publication for which these data were generated[3].

35. Csárdi, G. & Nepusz, T. The igraph software package for complex network research. *InterJournal, Complex Systems* **1695**, 1695 (2006).
36. Aulchenko, Y.S., Ripke, S., Isaacs, A. & van Duijn, C.M. GenABEL: an R library for genome-wide association analysis. *Bioinformatics* **23**, 1294–1296 (2007).
37. Smyth, G.K. Generalized linear models with varying dispersion. *J. R. Stat. Soc. B* **51**, 47–60 (1989).

© 2017 Nature America, Inc., part of Springer Nature. All rights reserved.